

Supporting Information

Structural Deformation and Host-Guest Properties of Doubly-Reduced Cycloparaphenylenes, [n]CPPs²⁻ (n = 6, 8, 10, and 12)

Zheng Zhou,^a Zheng Wei,^a Tobias A. Schaub,^b Ramesh Jasti,^{b,*} Marina A. Petrukhina^{a,*}

^a Department of Chemistry, University at Albany, State University of New York, Albany, NY 12222, USA

^b Department of Chemistry & Biochemistry, Materials Science Institute, and Knight Campus for Accelerating Scientific Impact, University of Oregon, Eugene, OR 97403, USA

I. Materials and Methods	S3
[[K ⁺ (18-crown-6)(THF)] ₂ ([8]CPP ²⁻)] (1)	S3
[[K ⁺ (18-crown-6)] ₂ ([10]CPP ²⁻)]·2THF (2 ·2THF)	S3
[K ⁺ (benzo-15-crown-5)] ₂ ([12]CPP ²⁻)·7THF (3 ·7THF)	S4
II. UV-Vis Spectroscopic Investigation	S4
Figure S1. UV-Vis spectra of [8]CPP/K/18-crown-6 in THF	S4
Figure S2. UV-Vis spectra of [10]CPP/K/18-crown-6 in THF	S5
Figure S3. UV-Vis spectra of [12]CPP/K/benzo-15-crown-5 in THF	S5
Figure S4. UV-Vis spectra of 1–3 crystals dissolved in THF	S6
III. Crystal Structure Solution and Refinement Details	S7
Table S1. Crystal data and structure refinement parameters for 1 , 2 , and 3	S8
Figure S5. ORTEP drawing of the asymmetric unit of 1	S9
Figure S6. ORTEP drawing of the asymmetric unit of 2	S9
Figure S7. ORTEP drawing of the asymmetric unit of 3	S10
Figure S8. C–H···π interactions in 1	S10
Figure S9. C–H···π interactions in 2	S11
Figure S10. C–H···π interactions in 3	S11
Table S2. Selected C–C distances (Å) of [8]CPP and [8]CPP ²⁻ in 1	S12
Table S3. Selected C–C distances (Å) of [10]CPP and [10]CPP ²⁻ in 2	S13
Table S4. Selected C–C distances (Å) of [12]CPP and [12]CPP ²⁻ in 3	S14
Figure S11. Dihedral angle calculation	S15
Figure S12. Calculation of d _A and d _{max} parameters	S15
IV. ¹H NMR Spectroscopic Investigation	S16
Figure S13. ¹ H NMR spectra of [8]CPP and <i>in situ</i> generated [8]CPP ²⁻ in the presence of 18-crown-6 in THF- <i>d</i> ₈	S16

Figure S14. ^1H NMR spectra of [10]CPP and *in situ* generated [10]CPP $^{2-}$ in the presence of 18-crown-6 in THF- d_8 S16

Figure S15. ^1H NMR spectra of [12]CPP and *in situ* generated [12]CPP $^{2-}$ in the presence of 18-crown-6 in THF- d_8 S17

Figure S16. ^1H NMR spectra of [12]CPP and *in situ* generated [12]CPP $^{2-}$ in the presence of benzo-15-crown-5 in THF- d_8 S17

V. References S18

I. Materials and Methods.

All manipulations were carried out using break-and-seal^[1] and glove-box techniques under an atmosphere of argon. Tetrahydrofuran (THF) was purchased from Sigma Aldrich, dried over Na/benzophenone, and distilled prior to use. Potassium metal (98%), 18-crown-6 ether (99%), and benzo-15-crown-5 ether (98%) were purchased from Sigma Aldrich and used as received. Tetrahydrofuran-*d*₈ (Sigma Aldrich) was dried over NaK₂ alloy and distilled prior to use. The samples of [8]CPP (C₄₈H₃₂), [10]CPP (C₆₀H₄₀), and [12]CPP (C₇₂H₄₈) were synthesized according to the previously reported procedures.^[2] The UV-Vis spectra were recorded on a PerkinElmer Lambda 35 spectrometer. The ¹H NMR spectra were measured using Bruker Ascend-500 spectrometer with a 5 mm BBO probe and referenced to the resonances of the solvent used. The low-temperature NMR experiments were controlled by a Cryo Diffusion cryogenic tank probe, and liquid N₂ was used as a cooling source. The temperature correction for -80 °C was calibrated by pure MeOH.

[{K⁺(18-crown-6)(THF)}₂([8]CPP²⁻)] (1)

THF (1.0 mL) was added to an NMR ampule (O.D. 4 mm) containing excess K (1.2 mg, 0.031 mmol, 20 eq.), [8]CPP (1.0 mg, 0.0016 mmol), and 18-crown-6 ether (1.0 mg, 0.0038 mmol). The ampule was sealed under argon and placed at 25 °C. The initial color of the mixture was yellow (neutral ligand), then it changed to brown after 4 hours and deepened to purple after 7 hours. Multiple black blocks were deposited along the walls of the ampule in moderate yield (*ca.* 60%) after 6 days. UV-Vis (THF, nm): λ_{max} 365, 585.

[{K⁺(18-crown-6)}₂([10]CPP²⁻)]·2THF (2·2THF)

THF (1.2 mL) was added to an NMR ampule (O.D. 5 mm) containing excess K (1.5 mg, 0.038 mmol, 25 eq.), [10]CPP (1.0 mg, 0.0015 mmol), and 18-crown-6 ether (1.6 mg, 0.006 mmol). The ampule was sealed under argon and placed at 25 °C. The initial color of the mixture was pale yellow (neutral ligand), then it changed to brown after 3 hours, and deepened to purple after 6 hours. Large black plates were deposited along the walls of the ampule in moderate yield (*ca.* 55%) after one week. UV-Vis (THF, nm): λ_{max} 361, 590.

[K⁺(benzo-15-crown-5)₂]₂([12]CPP²⁻)·7THF (3·7THF)

THF (0.6 mL) was added to an NMR ampule (O.D. 5mm) containing excess K (1.3 mg, 0.033 mmol, 15 eq.), [12]CPP (2 mg, 0.0022 mmol) and benzo-15-crown-5 ether (1.2 mg, 0.0045 mmol). The ampule was sealed under argon and placed at 25 °C. The initial color of the mixture was off-white (neutral ligand), then it changed to blue after 2 hours, and deepened to purple after 4 hours. Small purple plate-shaped crystals were deposited along the walls of the ampule in moderate yield (*ca.* 50%) after 6 days. UV-Vis (THF, nm): λ_{max} 346, 573.

II. UV-Vis Spectroscopic Investigation

Sample preparation: THF (2 mL) was added to a glass ampule (O.D. 10 mm) containing excess K (0.2 mg, ~30-50 eq.) and ~0.2 mg of [8]CPP, [10]CPP, or [12]CPP (1.6×10^{-4} mmol, 1.3×10^{-4} mmol, and 1.1×10^{-4} mmol, respectively). The ampule was sealed under argon and UV-Vis spectra were monitored at different reaction times (total 24 hours) at room temperature.

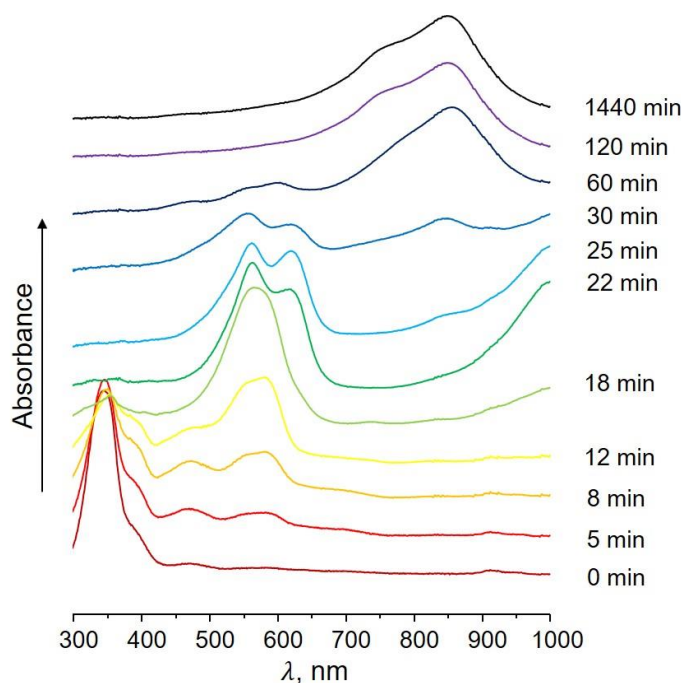


Figure S1. UV-Vis spectra of [8]CPP/K/18-crown-6 in THF.

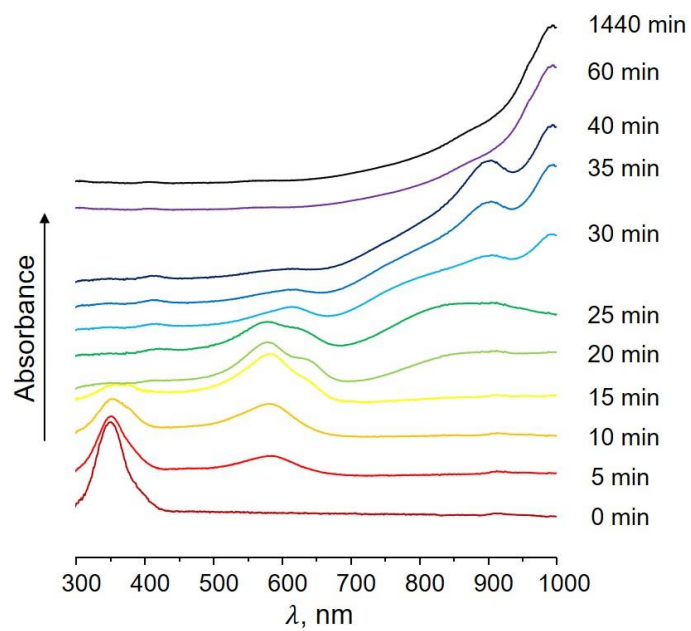


Figure S2. UV-Vis spectra of [10]CPP/K/18-crown-6 in THF.

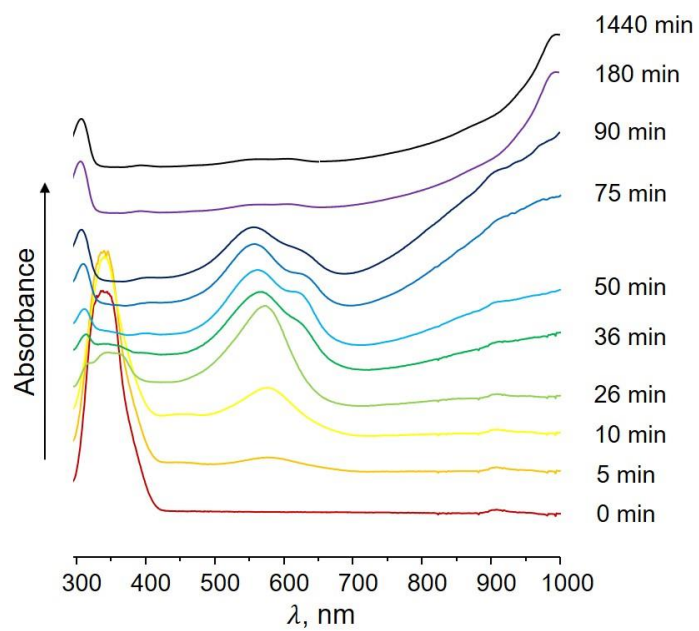


Figure S3. UV-Vis spectra of [12]CPP/K/benzo-15-crown-5 in THF.

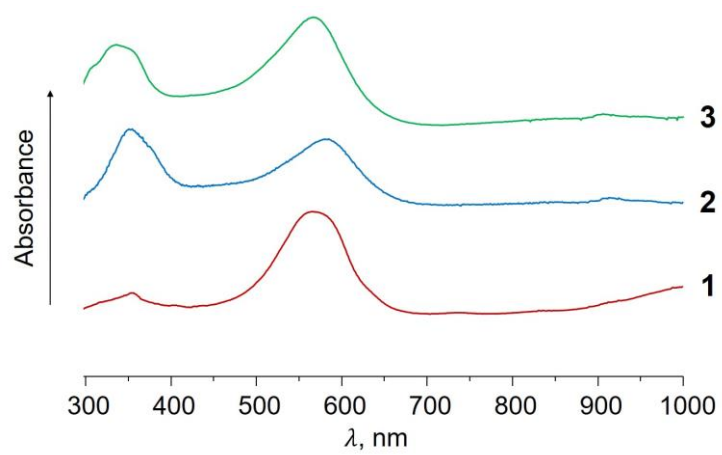


Figure S4. UV-Vis spectra of **1–3** crystals dissolved in THF.

III. Crystal Structure Solution and Refinement Details

Data collections of **1** and **2**·2THF were performed on a Bruker D8 VENTURE X-ray diffractometer equipped with a PHOTON 100 CMOS detector and a Mo-target X-ray tube ($\lambda = 0.71073 \text{ \AA}$) at 100(2) K. Both data were collected at 50 kV and 30 mA with an appropriate $0.5^\circ \omega$ scan strategy. Data collection of **3**·7THF was performed at 100(2) K on a Bruker D8 diffractometer, which is integrated with a Pilatus $3 \times 2\text{M}$ detector and modified for synchrotron use at the ChemMatCARS 15-ID-B beamline at the Advanced Photon Source (Argonne National Laboratory). Synchrotron diffraction data were collected at 20 keV ($\lambda = 0.61992 \text{ \AA}$) with $0.5^\circ \phi$ scan strategy, while manually attenuating the beam to minimize overages of individual pixels. Data reduction and integration were performed with the Bruker software package SAINT (version 8.37A).^[3] Data were corrected for absorption effects using the empirical methods as implemented in SADABS (version 2016/2).^[4] The structures were solved by SHELXT (version 2018/2)^[5] and refined by full-matrix least-squares procedures using the Bruker SHELXTL (version 2018/3)^[6] software package. All non-hydrogen atoms (including those in disorder parts) were refined anisotropically. The H-atoms were also included at calculated positions and refined as riders, with $U_{\text{iso}}(\text{H}) = 1.2 U_{\text{eq}}(\text{C})$. In **1**, the coordinated THF molecule was found to be disordered; and the disorder was modeled with two orientations with relative occupancies of 0.55:0.45 for the two parts. The anisotropic displacement parameters of the whole molecule in the direction of the bonds were restrained to be equal with a standard uncertainty of 0.004 \AA^2 . They were also restrained to have the same U_{ij} components, with a standard uncertainty of 0.01 \AA^2 . In **2**·2THF, the solvated THF molecule was found to be disordered and modeled with two orientations having relative occupancies of 0.81:0.19. The geometries of the disordered parts were restrained to be similar. The anisotropic displacement parameters of the disordered molecules in the direction of the bonds were restrained to be equal using RIGU command with default standard uncertainty. They were also restrained to have the same U_{ij} components using SIMU with standard uncertainty of 0.01. In **3**·7THF, the anisotropic displacement parameters of the [12]CPP ring in the direction of the bonds were restrained to be equal with a standard uncertainty of 0.004 \AA^2 . They were also restrained to have the same U_{ij} components, with a standard uncertainty of 0.01 \AA^2 . In each unit cell, five THF solvent molecules were found to be severely disordered and thus removed by the OLEX2's solvent mask.^[6-7] The total void volume was 642.2 \AA^3 , equivalent to 19.57% of the unit cell's total volume. Further crystal and data collection details are listed in Table S1.

Table S1. Crystal data and structure refinement parameters for **1**, **2**·2THF, and **3**·7THF.

Compound	1	2 ·2THF	3 ·7THF
Empirical formula	C ₈₀ H ₉₆ K ₂ O ₁₄	C ₉₂ H ₁₀₄ K ₂ O ₁₄	C ₁₅₆ H ₁₈₄ K ₂ O ₂₇
Formula weight	1359.76	1511.95	2569.22
Temperature (K)	100(2)	100(2)	100(2)
Wavelength (Å)	0.71073	0.71073	0.61992
Crystal system	Monoclinic	Orthorhombic	Triclinic
Space group	<i>P2/c</i>	<i>Pbca</i>	<i>P</i> -1
<i>a</i> (Å)	10.0128(19)	16.9050 (16)	13.3620(5)
<i>b</i> (Å)	19.991(4)	18.2916 (17)	14.3577(5)
<i>c</i> (Å)	18.021(3)	24.694 (2)	19.7293(7)
α (°)	90.00	90.00	104.7300(10)
β (°)	100.403(2)	90.00	103.0350(10)
γ (°)	90.00	90.00	108.1510(10)
<i>V</i> (Å ³)	3548.0(12)	7635.8 (12)	3281.6(2)
<i>Z</i>	2	4	1
ρ_{calcd} (g·cm ⁻³)	1.273	1.315	1.300
μ (mm ⁻¹)	0.199	0.19	0.108
<i>F</i> (000)	1452	3224	1374
Crystal size (mm)	0.06×0.12×0.16	0.22×0.13×0.06	0.002×0.005×0.006
θ range for data collection (°)	2.90–26.43	2.80–25.40	2.53–24.47
Reflections collected	78253	133578	56692
Independent reflections	7296	7011	10827
	[<i>R</i> _{int} = 0.0809]	[<i>R</i> _{int} = 0.0147]	[<i>R</i> _{int} = 0.0419]
Transmission factors (min/max)	0.6029/0.6629	0.5485/0.5877	0.6084/0.7309
Data/restraints/params.	7296/220/479	7011/232/533	10827/542/721
<i>R</i> 1, ^a <i>wR</i> 2 ^b (<i>I</i> > 2 σ (<i>I</i>))	0.0541, 0.0971	0.0698, 0.1308	0.0794, 0.2462
<i>R</i> 1, ^a <i>wR</i> 2 ^b (all data)	0.0891, 0.1099	0.1086, 0.1455	0.0852, 0.2534
Quality-of-fit ^c	1.067	1.089	1.080

^a*R*1 = $\Sigma||F_o| - |F_c|| / \Sigma|F_o|$. ^b*wR*2 = $[\Sigma[w(F_o^2 - F_c^2)^2] / \Sigma[w(F_o^2)^2]]$.

^cQuality-of-fit = $[\Sigma[w(F_o^2 - F_c^2)^2] / (N_{\text{obs}} - N_{\text{params}})]^{1/2}$, based on all data.

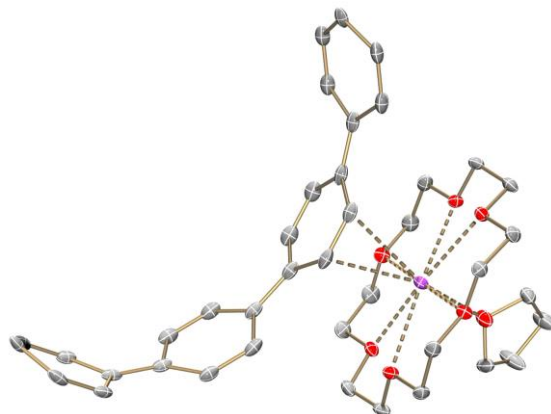


Figure S5. ORTEP drawing of the asymmetric unit of **1** with thermal ellipsoids at the 40% probability level. H atoms are removed for clarity. Color scheme used: K dark orchid, C gray, O red.

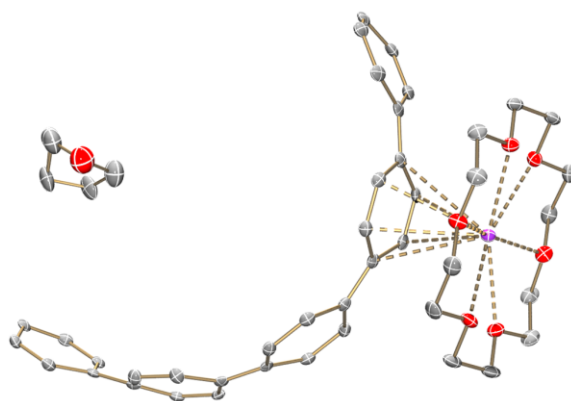


Figure S6. ORTEP drawing of the asymmetric unit of **2·2THF** with thermal ellipsoids at the 40% probability level. H atoms are removed for clarity. Color scheme used: K dark orchid, C gray, O red.

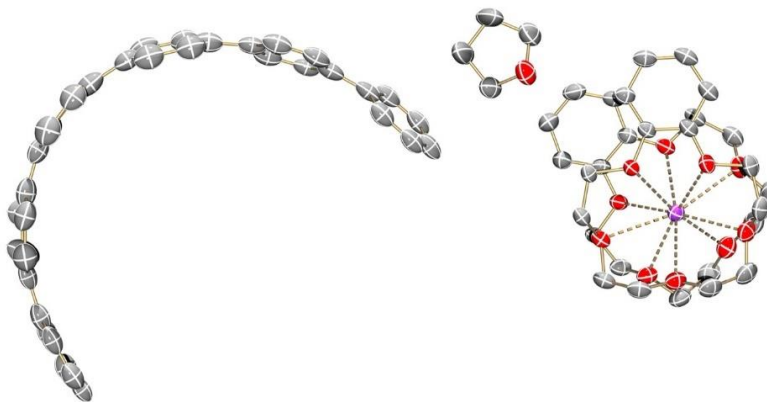


Figure S7. ORTEP drawing of the asymmetric unit of **3·7THF**, drawn with thermal ellipsoids at the 40% probability level. H atoms are omitted for clarity. Five highly disordered THF molecules were removed during structure refinement, while two remaining THF molecules were refined anisotropically. The color scheme used: C grey, H white, O red, and K dark orchid.

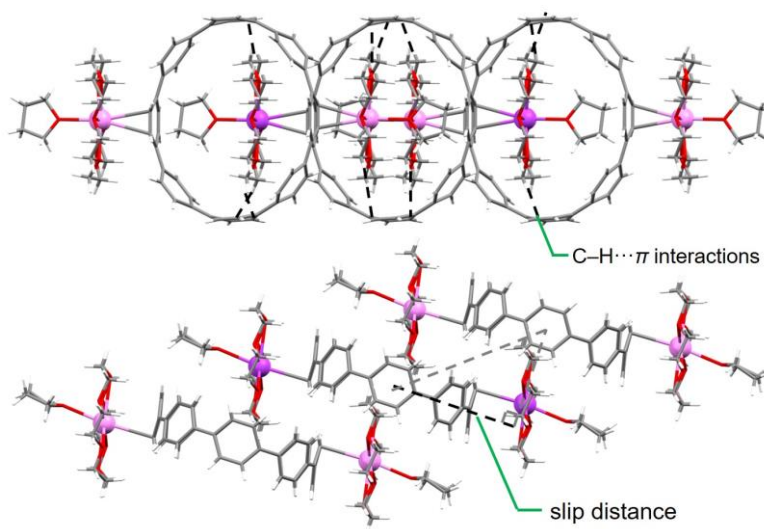


Figure S8. C–H··· π interactions and slip distance between neighboring molecules in **1**, face and side views, mixed models. K⁺ ions from different molecules are shown in different shades of purple.

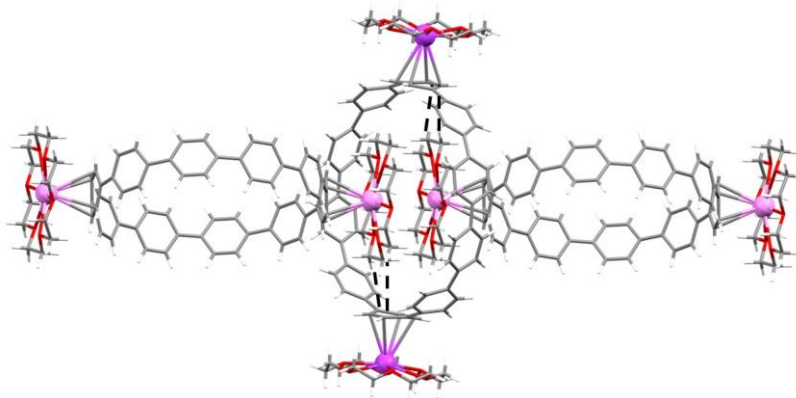


Figure S9. C–H··· π interactions between three neighboring molecules in **2**, mixed model. K^+ ions from different molecules are shown in different shades of purple.

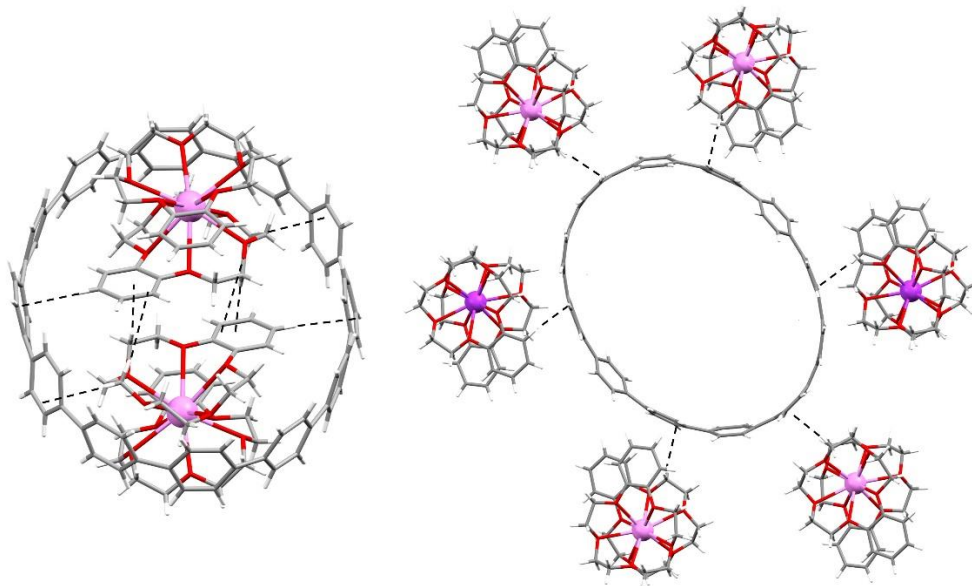
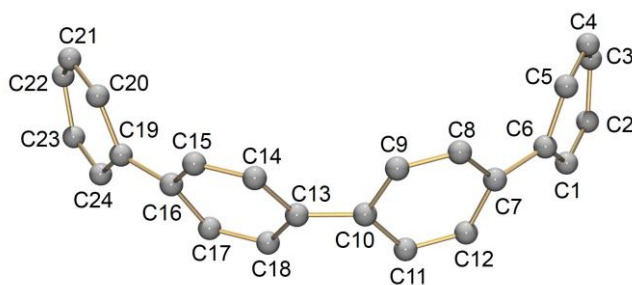
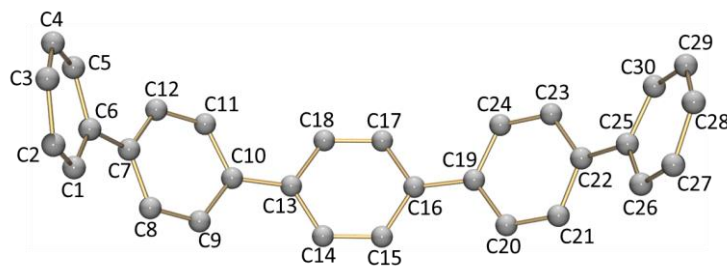


Figure S10. C–H··· π interactions in **3** between the internal cavity (left) or external surface (right) of the $[12]CPP^{2-}$ dianion and the $\{K^+(\text{benzo-15-crown-5})\}$ moieties from the adjacent units, mixed models. K^+ ions from adjacent molecules are shown in pink.

Table S2. Selected C–C distances (Å) of [8]CPP and [8]CPP²⁻ in **1**, along with labeling scheme.

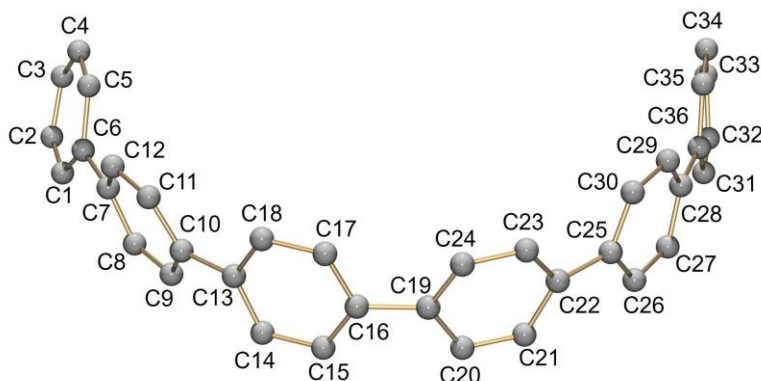
Distance	[8]CPP ^[2]	[8]CPP ²⁻	Distance	[8]CPP ^[2]	[8]CPP ²⁻
C1–C2	1.383(2)	1.361(4)	C11–C12	1.386(2)	1.370(4)
C1–C6	1.399(2)	1.423(3)	C13–C14	1.399(2)	1.419(3)
C2–C3	1.400(2)	1.430(3)	C13–C18	1.402(2)	1.419(3)
C3–C4	1.401(2)	1.423(3)	C14–C15	1.382(2)	1.365(4)
C3–C22	1.490(2)	1.438(4)	C15–C16	1.406(2)	1.412(3)
C4–C5	1.384(2)	1.364(5)	C16–C17	1.400(2)	1.421(3)
C5–C6	1.403(2)	1.425(3)	C16–C19	1.486(2)	1.447(4)
C6–C7	1.486(2)	1.436(4)	C17–C18	1.385(2)	1.372(4)
C7–C8	1.402(2)	1.417(3)	C19–C20	1.401(2)	1.424(3)
C7–C12	1.403(2)	1.422(3)	C19–C24	1.401(2)	1.419(3)
C8–C9	1.377(2)	1.366(4)	C20–C21	1.383(2)	1.365(4)
C9–C10	1.402(2)	1.418(3)	C21–C22	1.402(2)	1.416(3)
C10–C11	1.400(2)	1.410(3)	C22–C23	1.402(2)	1.427(3)
C10–C13	1.481(2)	1.449(4)	C23–C24	1.383(2)	1.365(4)

Table S3. Selected C–C bond distances (Å) [10]CPP and [10]CPP²⁻ in **2**, along with labeling scheme.



Distance	[10]CPP ^[2]	[10]CPP ²⁻	Distance	[10]CPP ^[2]	[10]CPP ²⁻
C1–C2	1.385(2)	1.378(5)	C15–C16	1.407(2)	1.409(5)
C1–C6	1.400(2)	1.404(5)	C16–C17	1.394(2)	1.417(5)
C2–C3	1.402(2)	1.409(5)	C16–C19	1.476(2)	1.462(5)
C3–C4	1.396(2)	1.413(5)	C17–C18	1.388(2)	1.369(5)
C3–C28	1.485(2)	1.455(5)	C19–C20	1.402(2)	1.410(5)
C4–C5	1.384(2)	1.373(5)	C19–C24	1.402(2)	1.410(5)
C5–C6	1.402(2)	1.416(5)	C20–C21	1.388(2)	1.369(5)
C6–C7	1.485(2)	1.448(5)	C21–C22	1.394(2)	1.413(5)
C7–C8	1.398(2)	1.413(5)	C22–C23	1.403(2)	1.406(5)
C7–C12	1.399(2)	1.413(5)	C22–C25	1.486(2)	1.456(5)
C8–C9	1.383(2)	1.375(5)	C23–C24	1.383(2)	1.371(5)
C9–C10	1.395(2)	1.422(5)	C25–C26	1.400(2)	1.403(5)
C10–C11	1.410(2)	1.410(5)	C25–C30	1.396(2)	1.412(5)
C10–C13	1.483(2)	1.443(5)	C26–C27	1.387(2)	1.375(5)
C11–C12	1.385(2)	1.368(5)	C27–C28	1.400(2)	1.408(5)
C13–C14	1.399(2)	1.416(5)	C28–C29	1.401(2)	1.412(5)
C13–C18	1.400(2)	1.414(5)	C29–C30	1.385(2)	1.364(5)
C14–C15	1.375(2)	1.376(5)			

Table S4. Selected C–C bond distances (Å) [12]CPP and [12]CPP²⁻ in **3**, along with labeling scheme.



Distance	[12]CPP ^[8]	[12]CPP ²⁻	Distance	[12]CPP ^[8]	[12]CPP ²⁻
C1–C2	1.376(5)	1.365(7)	C17–C18	1.372(5)	1.409(8)
C1–C6	1.390(5)	1.400(7)	C19–C20	1.396(5)	1.369(7)
C2–C3	1.400(5)	1.402(6)	C19–C24	1.399(5)	1.367(7)
C3–C4	1.394(5)	1.385(6)	C20–C21	1.391(5)	1.384(8)
C3–C34	1.483(5)	1.468(7)	C21–C22	1.394(5)	1.394(7)
C4–C5	1.381(5)	1.392(7)	C22–C23	1.394(5)	1.378(7)
C5–C6	1.400(5)	1.377(6)	C22–C25	1.485(5)	1.473(7)
C6–C7	1.477(5)	1.474(7)	C23–C24	1.382(5)	1.388(8)
C7–C8	1.404(5)	1.357(7)	C25–C26	1.387(6)	1.399(6)
C7–C12	1.395(5)	1.379(7)	C25–C30	1.374(6)	1.373(6)
C8–C9	1.377(5)	1.387(8)	C26–C27	1.372(5)	1.368(7)
C9–C10	1.406(5)	1.370(7)	C27–C28	1.391(5)	1.389(6)
C10–C11	1.391(5)	1.351(7)	C28–C29	1.375(5)	1.374(6)
C10–C13	1.478(5)	1.476(8)	C28–C31	1.488(5)	1.455(7)
C11–C12	1.392(5)	1.368(8)	C29–C30	1.385(6)	1.384(7)
C13–C14	1.390(5)	1.397(7)	C31–C32	1.399(4)	1.378(6)
C13–C18	1.414(5)	1.376(7)	C31–C36	1.418(9)	1.413(6)
C14–C15	1.385(5)	1.376(8)	C32–C33	1.405(5)	1.404(7)
C15–C16	1.394(5)	1.376(7)	C33–C34	1.381(4)	1.369(6)
C16–C17	1.396(5)	1.331(7)	C34–C35	1.390(9)	1.387(6)
C16–C19	1.480(5)	1.499(8)	C35–C36	1.360(11)	1.367(7)

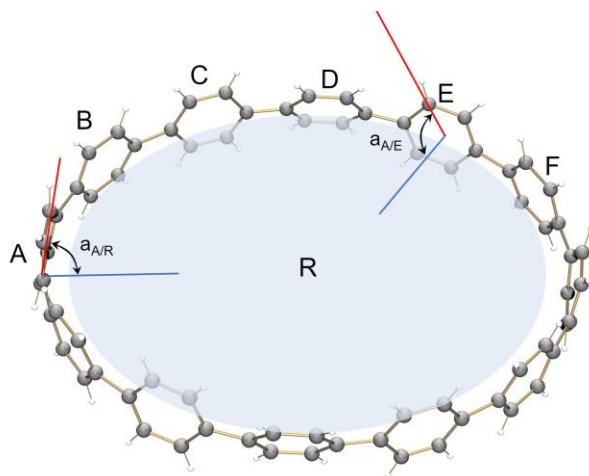


Figure S11. Dihedral angle calculation. Plane R is formed by all bridging C-atoms in CPP, and the dihedral angle between the plane R and the plane of each six-membered ring (A–F) is calculated.

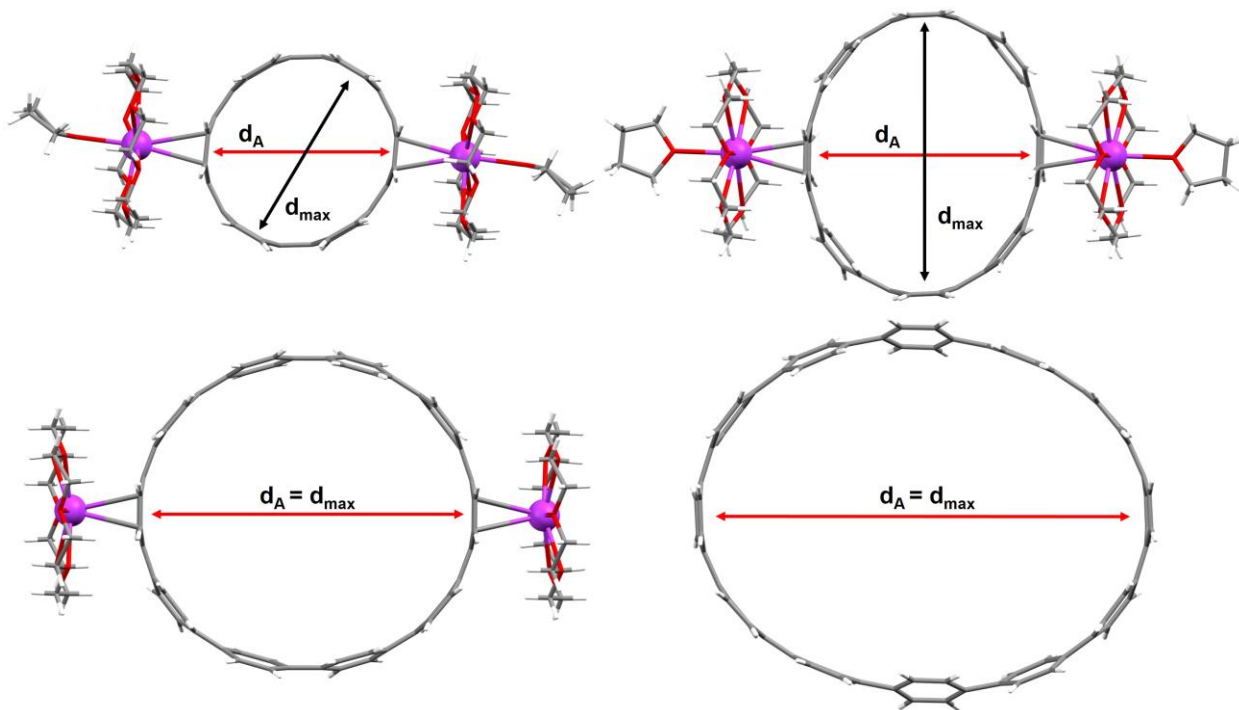


Figure S12. Calculation of d_A and d_{max} parameters.

Note: For contact-ion complexes, the d_A direction of the CPP dianions is the same as the axis going through two K^+ ions; for the solvent-separated $[12]CPP^{2-}$ anion, d_A is d_{max} .

IV. ^1H NMR Spectroscopic Investigation

Sample preparation: THF- d_8 (0.6 mL) was added to an NMR tube (O.D. 5 mm) containing $[n]\text{CPP}$ ($n = 8, 10,$ and 12) (2 mg, 0.0032 mmol, 0.0030 mmol, 0.0022 mmol, respectively), excess K (2 mg, 0.051 mmol), and 18-crown-6 (2 mg, 0.0075 mmol) or benzo-15-crown-5 (1 mg, 0.045 mmol), and the tube was sealed under argon.

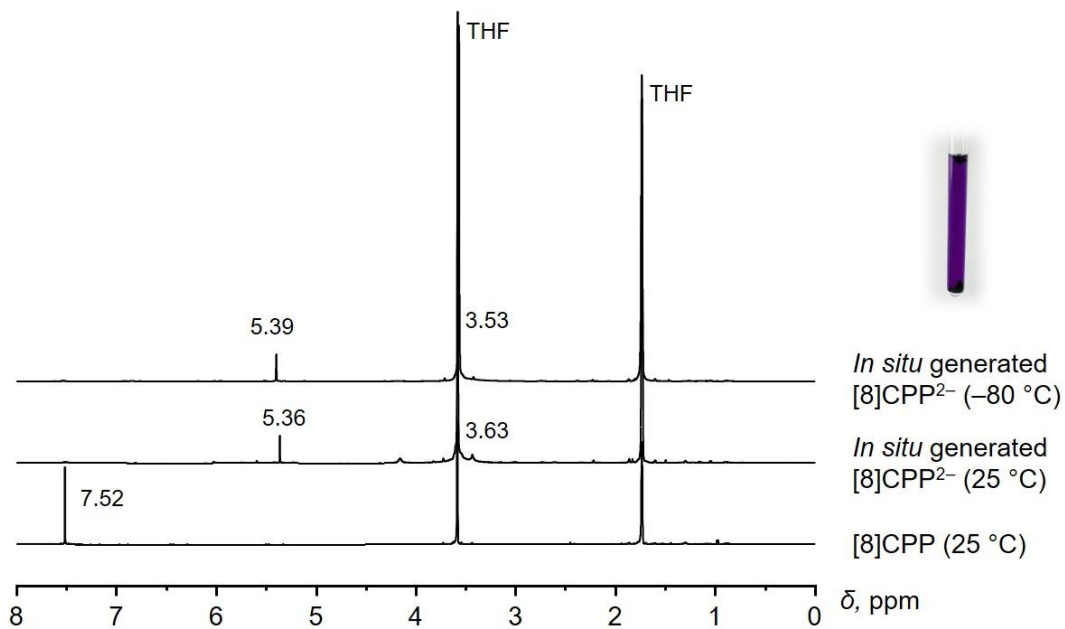


Figure S13. ^1H NMR spectra of [8]CPP and *in situ* generated [8]CPP $^{2-}$ in the presence of 18-crown-6 in THF- d_8 .

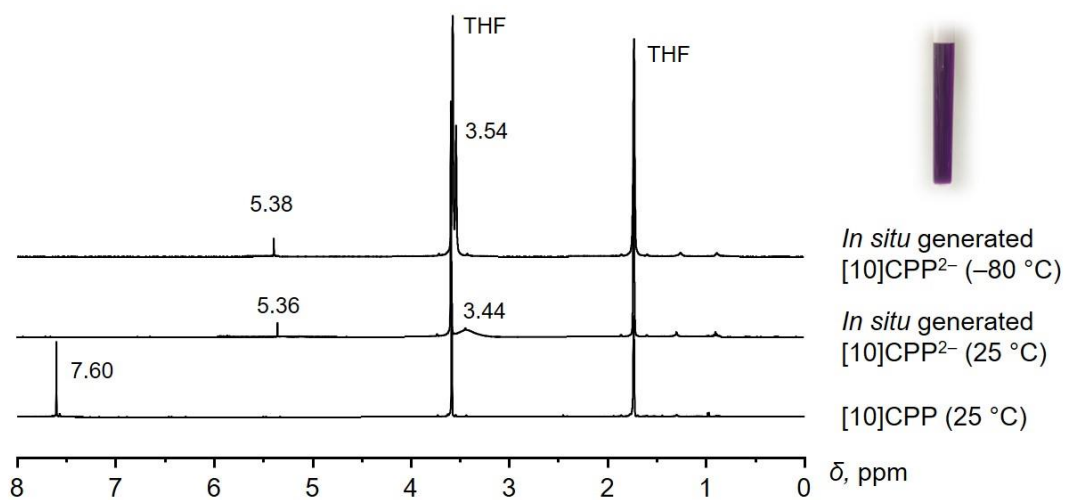


Figure S14. ^1H NMR spectra of [10]CPP and *in situ* generated [10]CPP $^{2-}$ in the presence of 18-crown-6 in THF- d_8 .

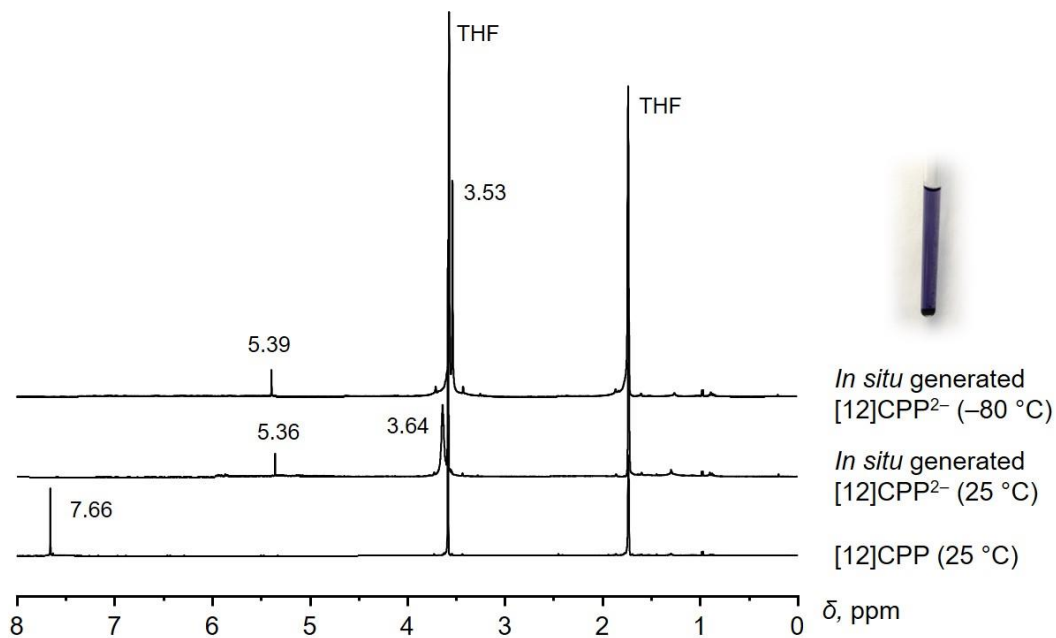


Figure S15. ¹H NMR spectra of [12]CPP and *in situ* generated [12]CPP²⁻ in the presence of 18-crown-6 in THF-*d*₈.

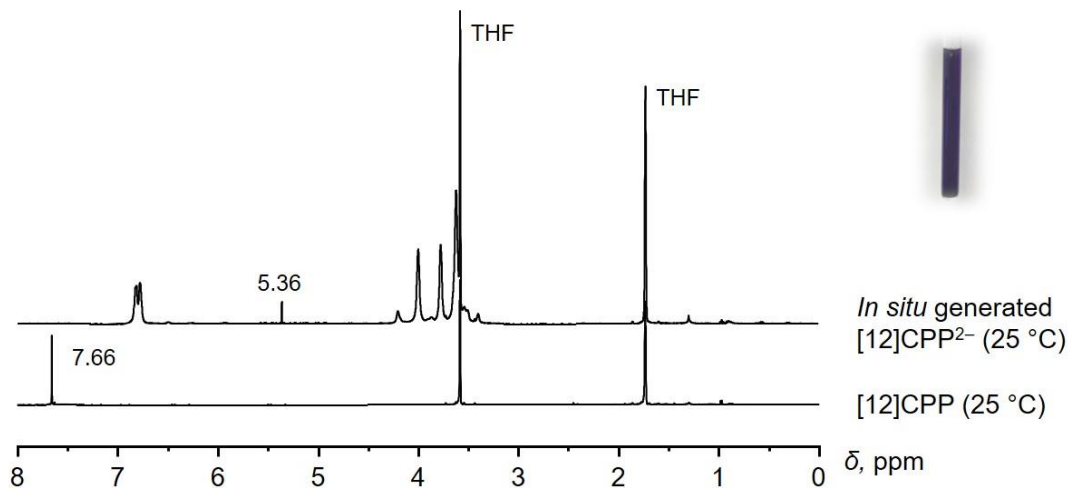


Figure S16. ¹H NMR spectra of [12]CPP and *in situ* generated [12]CPP²⁻ in the presence of benzo-15-crown-5 in THF-*d*₈.

V. References

- [1] N. V. Kozhemyakina, J. Nuss, M. Jansen, *Z. Anorg. Allg. Chem.* **2009**, *635*, 1355-1361.
- [2] J. Xia, J. W. Bacon, R. Jasti, *Chem. Sci.* **2012**, *3*, 3018-3021.
- [3] SAINT; part of Bruker APEX3 software package (version 2017.3-0): Bruker AXS, **2017**.
- [4] SADABS; part of Bruker APEX3 software package (version 2017.3-0): Bruker AXS, **2017**.
- [5] G. M. Sheldrick, *Acta Crystallogr.* **2015**, *A71*, 3-8.
- [6] G. M. Sheldrick, *Acta Crystallogr.* **2015**, *C71*, 3-8.
- [7] O. V. Dolomanov, L. J. Bourhis, R. J. Gildea, J. A. K. Howard, H. Puschmann, *J. Appl. Crystallogr.* **2009**, *42*, 339-341.
- [8] Y. Segawa, S. Miyamoto, H. Omachi, S. Matsuura, P. Šenel, T. Sasamori, N. Tokitoh, K. Itami, *Angew. Chem. Int. Ed.* **2011**, *50*, 3244-3248.